Chemically Attaching Polyhydroxyethylmethacrylate Brush on Substrate Surface, Derivation, and the Role in Differential Etching

Feng Zhou, Zonggang Mu, Tingmei Wang, Zhilu Liu, Bo Yu, Jingcheng Hao, Weimin Liu

State Key Laboratory of Solid Lubrication, Lanzhou Institute of Chemical Physics, Chinese Academy of Sciences, Lanzhou, People's Republic of China

Received 10 May 2004; accepted 10 September 2004
DOI 10.1002/app.25046
Published online 28 June 2007 in Wiley InterScience (www.interscience.wiley.com).

ABSTRACT: This article reports the preparation and derivation of chemically tethered polyhydroxyethylmethacrylate (PHEMA) brush and its application in microfabrication. PHEMA brush was prepared by the surface-initiated atomic transfer radical polymerization and derived by either organic reaction or sequence polymerization. The differential etching process was studied by atomic force microscope (AFM) and optical micrograph. PHEMA brush cannot prevent the underlying gold from dissolving in aqueous etchant KI/I_2 solution. Differential etching of UV-patterned PHEMA template resulted in metal (gold) rings.
© 2007 Wiley Periodicals, Inc. J Appl Polym Sci 106: 723–729, 2007

Key words: film; atomic force microscope (AFM); atomic transfer radical polymerization (ATRP); self-assembly; hydrophilic polymer

INTRODUCTION

Surface-initiated polymerization (SIP) provides an easy way to prepare densely packed and chemically tethered polymer brushes through *in situ* grafting polymer chains from substrate surfaces.[1–4] Modifications of inorganic substrates can be realized by SIP from self-assembled monolayers (SAMs) of initiator. SAM-amplified polymer brushes are usually characterized by improved mechanical property, anticorrosion, chemical versatility, etc.[5,6] compared with their SAMs counterparts.[7–9] For example, SAM often has the imperfect package arising from grain boundaries of substrate.[10–12] The resulted structural defects even a molecular missing can lead to etching resistance failure.[13,14] Therefore, it is still uncertain whether the SAMs can completely resist etching, especially when some special etchants were used.[15] Polymer brushes offer more versatility in this respect in that these defects can be screened by relatively long flexible polymer chains. Shah et al. examined the resistance, against various etchants, of a series of hydrophobic polymer brushes prepared by SIP and concluded that different polymer brushes had different etching resistant capability.[16] Huck et al. once used an ultrathin polymer film, prepared by a layer-by-layer assembly method, to resist the etching by ferricyanide. The method, however, suffers from too many reaction steps.[5] The SIP method can control the brush thickness in a wide range (from several nanometers to more than 100 nm) and a great variety of polymer brushes can be prepared according to actual needs. This article deals with the preparation of chemically tethered hydrophilic polyhydroxyethylmethacrylate (PHEMA) brush, its derivation, and the differential etching on it. Differential etching on PHEMA brush pattern has an unexpected result and gold rings were generated. The research may be of great importance in nano/micro fabrication in the aspect of resist-etchant design.

EXPERIMENTAL

Materials

Mercapto hexanol (Aldrich), 2-bromoisobutyryl bromide (BiBB, TCI), and 1H,2H,3H,4H-perfluoro octadecyl trichlorosilane (FOS, Aldrich) were used without further purification. Bipyridine, CuBr, and palmitoyl chloride (PC) were obtained from Shanghai Chemical Reagents Co. and used directly. Hydroxyethylmethacrylate (HEMA, Aldrich), glycidylmethacrylate (GMA, Aldrich), and methylmethacrylate (MMA, Shanghai Chemical Reagents Co., Shanghai, China) were vacuum distilled before use.

Correspondence to: F. Zhou (zhouf@ns.lzb.ac.cn).
Contract grant sponsor: National Science Foundation of China; contract grant number: 50272608.
Contract grant sponsor: Chinese Ministry of Science and Technology; contract grant number: 2002AA302609.
Contract grant sponsor: Top Hundreds Talent Program of Chinese Academy of Sciences; contract grant number: 50405040.

© 2007 Wiley Periodicals, Inc.
WILEY InterScience® DISCOVER SOMETHING GREAT

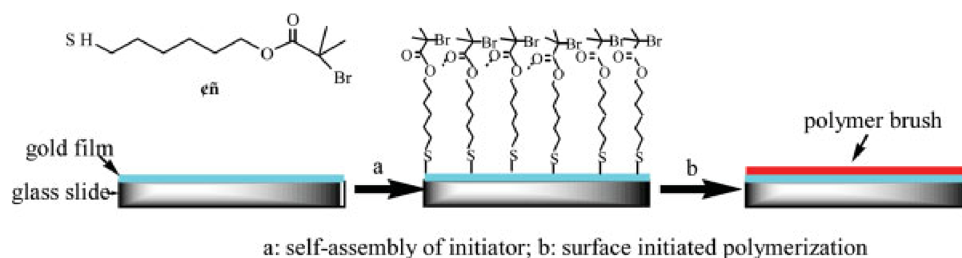

Scheme 1 Formation of initiator monolayer and surface-initiated atomic transfer radical polymerization. [Color figure can be viewed in the online issue, which is available at www.interscience.wiley.com.]

Synthesis and self-assembly of initiator ($Br(CH_3)_2CCOO(CH_2)_6SH$)

BiBB (2.30 g, 10 mmol) was dipped into a solution of 1.34 g (10 mmol) mercaptohexanol in dry THF cooled by ice water in the presence of 1.01 g (10 mmol) triethylamine. And then it was allowed to react completely for above 5 h at room temperature. The precipitate was filtered under a stream of N_2. The solvent in filtrate was removed to give initiator, followed by purification with aluminum column chromatography. The ultimate product is 0.97 g (yield: 34%). NMR (400 MHz, $CDCl_3$): 4.17 (t, 2H, OCH_2), 2.54 (q, 2H, SCH_2), 1.93 (s, 6H, CH_3), 1.60–1.68 (m, 4H, CH_2), 1.39–1.46 (m, 4H, CH_2); IR: 2958 cm^{-1} (νCH_3), 2926 and 2854 cm^{-1} (νCH_2), 1731 cm^{-1} (C=O). Assembly of initiator on gold film was realized by dipping vacuum-deposited gold film into 4 mmol L^{-1} ethanolic solution of initiator for above 24 h. The initiator monolayer-modified gold film was thoroughly rinsed by ethanol.

Preparation of polymer brush, derivation, and patterning

For a typical experiment, 1 mL monomer, 0.5 mmol CuBr, and 0.1 mmol bipyridine were mixed with 10 mL CH_3OH/H_2O (50/50 v/v) and deoxygenated for half an hour with a flow of N_2. After polymerization they were rinsed with methanol/water. Sequence polymerization was carried out under similar conditions, except that the solvent for MMA polymerization is (9/1 v/v) CH_3OH/H_2O. Derivation of PHEMA was carried out in vapor state of small molecules. Polymer brush was patterned with UV irradiation (125 W high-pressure Hg lamp) from a distance of 10 cm at a constant temperature of 30°. The etching rate of PHEMA is about 10 nm h^{-1}. For the sake of completely removing the exposed polymer brush, irradiation was prolonged for half an hour over the theoretical time.

Characterization

The static contact angle of distilled water on the film surface was measured on a CA-A contact angle meter. At least three points in different regions of the film surface were selected to carry out the measurements. The film thickness was determined on a Gaertner model L116C ellipsometer equipped with He–Ne laser (λ = 632.8 nm) at a fixed incidence angle of 70°. The attenuated total reflection infrared spectra (ATR-FTIR) were recorded on a Nicolet 870 infrared spectrometer equipped with a smart ATR accessory with 256 scans and a resolution of 4 cm^{-1}. The surface morphology was obtained by atomic force microscopy (AFM) using an SPM 9500 microscope (Shimazu).

RESULTS AND DISCUSSIONS

Preparation of PHEMA brush

The formation of initiator monolayer on gold film and surface-initiated atomic transfer radical polymerization (ATRP) are illustrated in Scheme 1. Self-assembly of initiator ($BrC(CH_3)_2COO(CH_2)_6SH$) on a vacuum-deposited gold film resulted in 1.1-nm-thick monolayer. The initiator monolayer showed a water contact angle of 96°. The chemically tethered PHEMA brushes are generated by polymerizing HEMA from

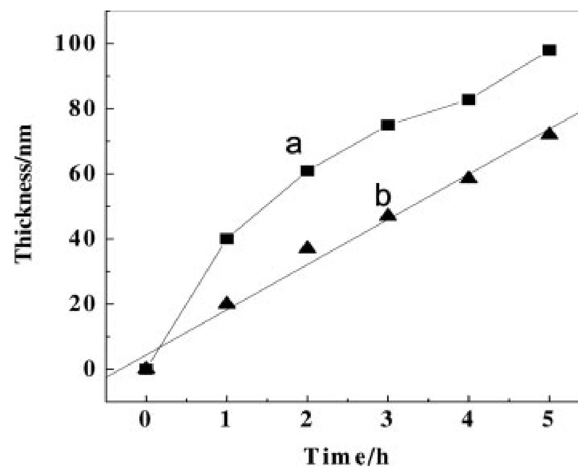

Figure 1 Variation of film thickness with polymerization time. (a) Without addition of $CuCl_2$; (b) addition of the equivalent molar $CuCl_2$.

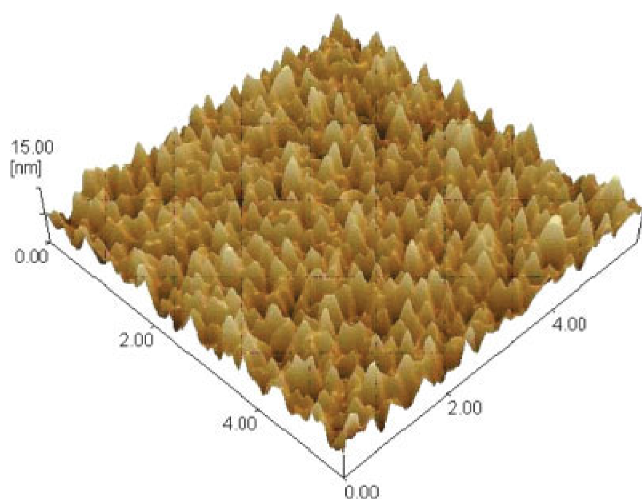

Figure 2 AFM morphology of PHEMA brush. [Color figure can be viewed in the online issue, which is available at www.interscience.wiley.com.]

the monolayer.[17] The water contact angle decreased to 42° after grafting of PHEMA layer, indicating that PHEMA film is a much hydrophilic surface because of the relative high surface energy induced by high density of hydroxyl groups. The variation of the thickness of PHEMA brush with the polymerization time is shown in Figure 1(a). Initially, the grafting polymerization of HEMA was very fast and gradually leveled off. Growth of PHEMA brush does not show a linear relationship with the polymerization time, which might be because of the low concentration of Cu (II) deactivator in polymerization system. When equivalent molar $CuCl_2$ with CuCl was added to the polymerization system, the thickness of PHEMA brush grew more linearly with the polymerization time, but a low growth rate compared with the cases of no addition of $CuCl_2$. This indicates that $CuCl_2$ can deactivate the initiation radical to a dormant state. AFM characterization of the obtained polymer brushes reveals that they are very homogeneous and smooth. A typical three-dimensional AFM morphology of the PHEMA brush is shown in Figure 2. It can be seen that the PHEMA brush is closely packed and has few defects, which is of very importance to the protection of the underlying surface.

The chemical composition of initiator monolayer and the PHEMA brush was characterized by XPS (Fig. 3). The absorbance peaks of C_{1s} and Br are

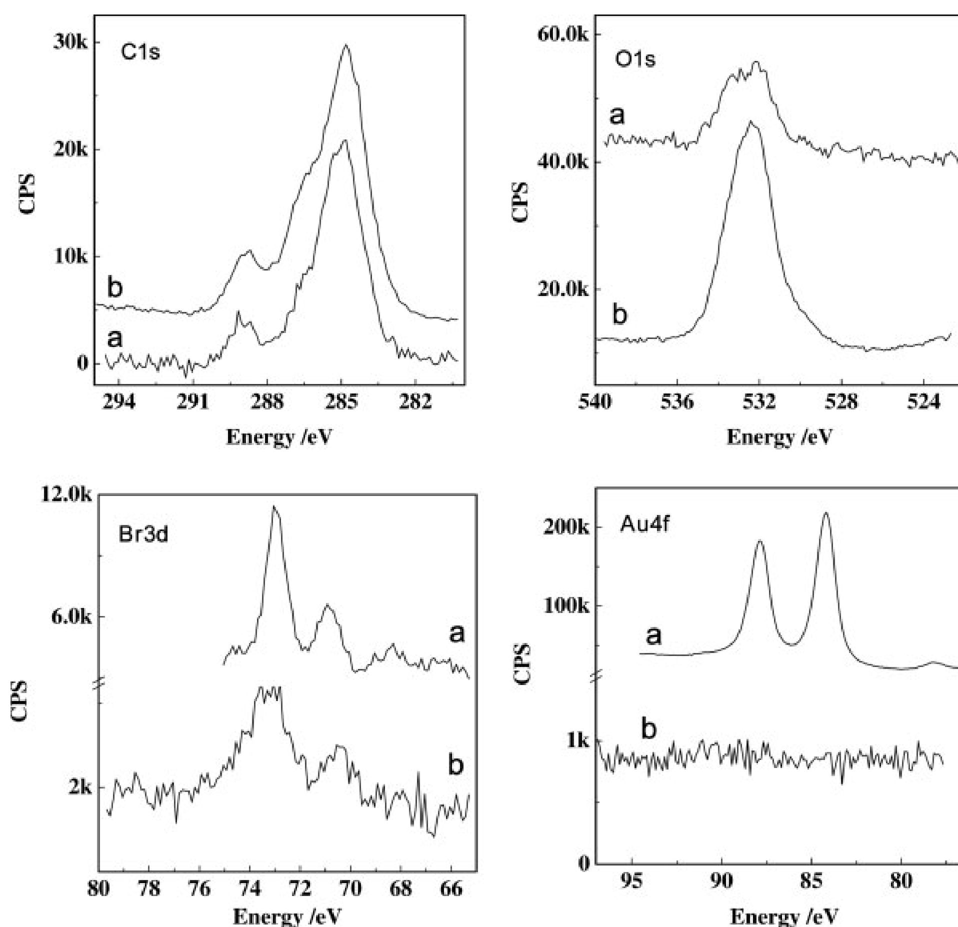

Figure 3 XPS spectra of the initiator monolayer (a) and 20-nm PHEMA brush (b).

similar before and after grafting PHEMA brush, but have different intensity. The absorbance peaks of C_{1s} at 285.0, 286.5, and 289.0 eV were attributed to *C—C, *C—O, *C= O. The absorbance peaks at 77.0 and 73.0 eV were ascribed to $Br3d_{3/2}$ and $Br3d_{1/2}$, respectively. The absorbance of O_{1s} for initiator monolayer was split into two peaks at 532.4 and 534.7 eV that correspond to C—O* (H—O*) and C=O* respectively, while the peaks at 534.7 eV becomes not so apparent for PHEMA brush due to the attenuation by C—O* and H—O*. The absorbance at 87.0 and 84.0 eV is attributed to Au4f, but completely disappeared for 20-nm-thick PHEMA brush. This indicates that the polymer brush was thick and homogeneous enough to block the excited Au4f electrons. It is worth noting that the Br signal can be easily detected after polymerization, only with the decreased intensity. Previous study using surface-initiated ATRP to graft copolymer brush proved the presence of end initiator moiety, but had no direct evidence.[18,19] This is the first time we use the XPS spectra to verify the existence of the initiating moiety at the end of polymer brush.

Derivation of PHEMA brush

Because of the living nature of ATRP and the functional hydroxyl groups of PHEMA, derivation of PHEMA brush can be realized through two ways: sequence polymerization resulting in copolymer brush and organic reaction of the hydroxyl groups with active molecules. We have detected, from XPS spectra, the presence of bromo group at the end of PHEMA brush. Therefore, it is possible for the terminal initiator moieties to re-initiate polymerization under ATRP conditions. The reactions are verified by the reflection FTIR spectra shown in Figure 4. For the 20-nm-thick PHEMA brush, the presence of the absorbance bands at 1730 cm^{-1} for C=O, 3000–2800 cm^{-1} for C—H, and the absorbance band with the central peak at 3400 cm^{-1} for hydroxyl group indicates successful grafting of PHEMA brush on the gold substrate. Copolymerization of HEMA from the PHEMA brush terminus was characterized by enlarged absorbance intensity of FTIR spectra [Fig. 4(b)] and increased brush thickness of about 90 nm after 24 h of polymerization (Table I). Brush growth speed from polymer brush layer cannot be comparable with that from initiator monolayer possibly because of the very low concentration of initiator moiety on polymer brush terminus. However, sequence polymerization of GMA was much easier because of the much higher initiation efficiency. A 24-h polymerization of GMA resulted in 170-nm PGMA adlayer (Table I). PHEMA-PGMA copolymer brush cannot display the absorbance of PHEMA in ATR-FTIR as can be viewed from the inexistence of the absorbance peaks of hydroxyl groups [Fig. 4(c)]. Copolymerization of MMA has the lowest film growth speed. Twenty-four-hours polymerization only resulted in 12-nm PMMA adlayer (Table I).

TABLE I
Derivation of PHEMA Brush by Sequence Polymerization and Organic Reaction

	Increased thickness (nm)	Contact angle
PHEMA[a]	90	42
PGMA[a]	170	57
MMA[a]	12	72
TMCS[b]	1.3	85
DCDMS[b]	5.4	83
FOS[b]	3.2	113
PC[b]	0.92	92
BiBB[b]	1.5	78

[a] Sequence polymerization for 24 h.
[b] Derivation by organic reaction.

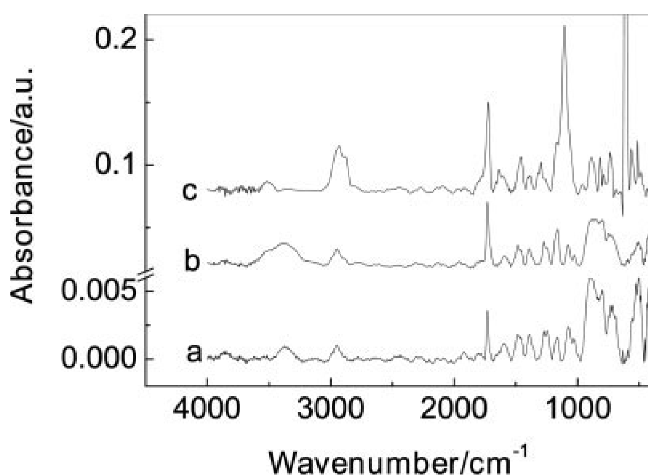

Figure 4 Reflection FTIR of 20-nm PHEMA brush (a), 90-nm PHEMA (b), and 170-nm PGMA (c) adlayer by sequence polymerization for 5 h.

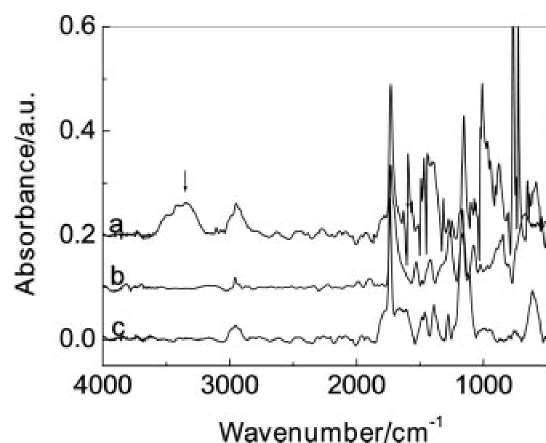

Figure 5 Reflection FTIR of 50-nm PHEMA brush (a), PHEMA brush derived by TMCS (b), and BiBB (c).

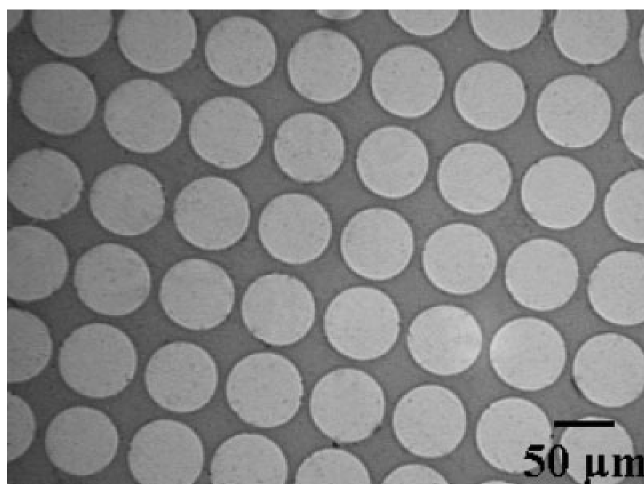

Figure 6 Optical micrograph of UV-patterned PHEMA brush template.

The free hydroxyl groups on the surface are liable to react with highly active molecules e.g., chlorosilane, carbonyl chloride, isocyanate, etc. Therefore, by simple organic reaction, the PHEMA brush can be derived and the surface wettability can be altered from the water contact angle measurement. Derivation of PHEMA brush by these molecules will modify not only the surface energy but also the thickness. After being treated with TMCS, thickness of PHEMA brush increased from 20 to 25.4 nm. The inconsistence of the increased thickness (5.4 nm) with the TMCS monolayer indicated the penetration of TMCS among PHEMA brush. The same can be seen with other modifications. Derivation reaction was verified by the disappearance of hydroxyl groups in FTIR spectra (Fig. 5). The re-attachment of initiator by reaction of hydroxyl groups with BiBB led to an increase of the contact angle to 78°. This indicates the successful attachment of initiator. The decrease of water contact angle compared with initiator monolayer is probably because of that BiBB molecules assume disordered orientations. The advantage of re-attachment of initiator moiety lies in that high-density initiator on PHEMA surface can be constructed again. Although the initiator moieties are still present after first ATRP, the residue terminal bromo groups are liable to decompose upon storage, resulting in dead ends that cannot re-initiate ATRP. Thus re-attaching initiator can ensure sequence polymerization at any time.

Differential wet chemical etching

The conventional photolithographic method is employed to generate the patterned polymer brush. Complete removal of polymer brush could be verified by ATR-FTIR. An optical micrograph of the UV-patterned 50-nm PHEMA brush is shown in Figure 6, where the UV etched area (bare gold) appears to be brighter, since gold has a higher reflection index than the polymer brush. The PHEMA pattern has very high edge resolution.

SAM-amplified polymer brush is often characterized by an improved etching resistant capability.[16] However, PHEMA shows nearly no etching resistance to KI/I_2 etchant. PHEMA-covered gold and the bare gold have the similar dissolving speed. The PHEMA-covered gold film is etched at an even higher speed than the exposed gold film. Figure 7(a) gives the AFM morphology of the PHEMA brush pattern after 50 s of etching. It can be seen that the exposed gold kept intact while the PHEMA brush was damaged to give rougher surface on PHEMA brush region. Figure 7(b) gives a close-up view of 7(a). It can be seen that a large number of etched pits appeared on PHEMA brush. This kind of differ-

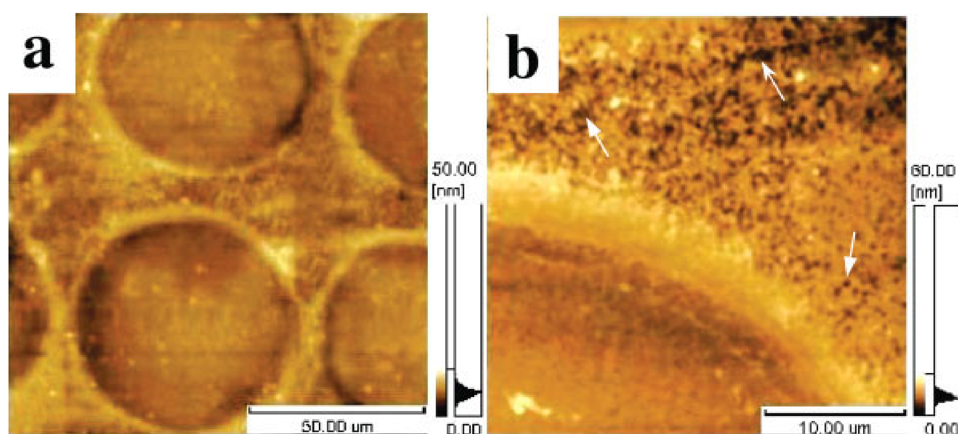

Figure 7 AFM morphology of PHEMA brush template after 50 s of etching. [Color figure can be viewed in the online issue, which is available at www.interscience.wiley.com.]

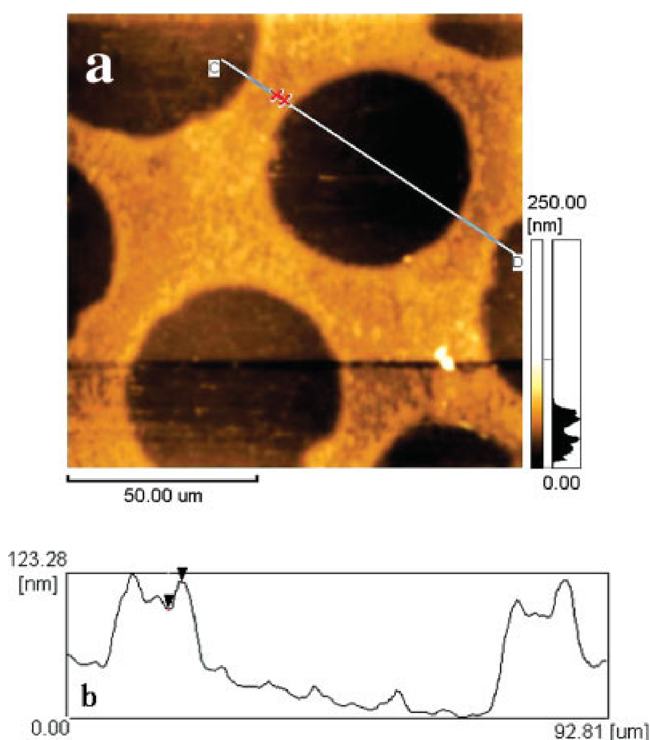

Figure 8 Camelback like microstructures obtained by differential etching for 60 s in KI/I_2 solution. [Color figure can be viewed in the online issue, which is available at www.interscience.wiley.com.]

ential etching was induced by different wettability of etchant solution on different regions.[20] The PHEMA brush is hydrophilic (with a water contact angle of 40°), and so can be wetted by the etchant solution. Then it may let the penetration of etchant and easy access to the sub gold layer, resulting in dissolving of gold film. Then PHEMA chains collapse to give a large number of etching pits, which in turn accelerates the dissolving of gold. Initially, KI/I_2 did not wet the bare gold at all because the bare gold surface is intrinsically hydrophobic (the water contact angle is 63°). So the bare gold was not destroyed at the beginning. On the other hand, irradiation of the PHEMA brush by the UV light might leave organic residues with stronger hydrophobicity than that of PHEMA in the exposed area. The etchant does not wet hydrophobic gold surface and residues. Therefore, the gold layer in the exposed area becomes more difficult to be etched.

From Figure 7 it can also be seen that the edge of PHEMA brush and the central region have different etching rates. AFM characterization of another sample after 60 s of etching showed that camelback like structures are generated as can be visualized from the depth profile along the marked line [Figs. 8(a) and 8 (b)]. The PHEMA brush collapsed for about 10 nm between the two-signed points. At this time the exposed gold still remains undisturbed.

Further increasing the etching time, the UV etched area began to be attacked by etchant. But to our surprise the edge gold between the exposed area and PHEMA-covered area had an even lower dissolving speed, the result of which was the generation of gold rings [Fig. 9(a)]. The exposed gold dissolved slowly. By further increasing the etching time, the gold rings became much thinner. An etching time of 2 min was adequate to completely remove the bare gold. By controlling the etching time, the feature size can be continuously reduced. This observation is just like anisotropic etching of Si (100) by the aqueous KOH solution in microfabrication that lateral dimension(s) between trenches can decrease in a controlled way as the etching proceeds. This technique is probably most useful for generating simple patterns of small-scale structures and in most cases must be combined with other techniques. Although these methods may lack the characteristics required for registration in device fabrication, they offer an easy access to small-scale structures that are directly useful in making sensors, arrays of nanoelectrodes, and diffraction gratings.

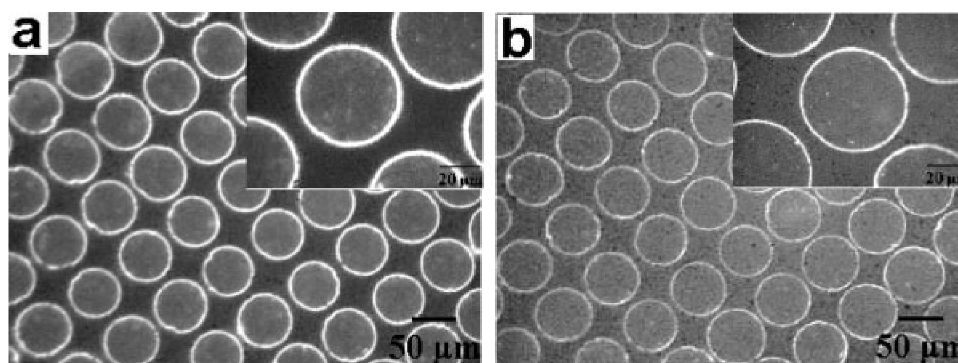

Figure 9 Optical micrographs of the obtained gold microstructures by etching PHEMA polymer brush pattern for different duration: (a) 80 s and (b) 110 s. The inserts are the magnified view.

CONCLUSIONS

Hydrophilic PHEMA brush on substrate surface was created through the surface-initiated ATRP. PHEMA brush can be derived by either sequence polymerization or the organic reaction between functional hydroxyl groups and active small molecules. Modification of PHEMA brush could alter the wettability from a hydrophilic surface to a hydrophobic one. PHEMA could not resist etching by KI/I_2 etchant solution. Therefore, differential etching of the UV-patterned hydrophilic PHEMA brush template gave gold rings. Thus, the method realizes size reduction and pattern alteration of original pattern. It is a novel addition to unconventional lithographic method and should find promising applications in fabricating NEMS/MEMS.

References

1. Zhao, B.; Brittain, W. J. Prog Polym Sci 2000, 25, 677.
2. Zhou, F.; Liu, W. M. Prog Chem 2002, 14, 141.
3. Castell, P.; Wouters, M.; de With, G.; Fischer, H.; Huijs, F. J Appl Polym Sci 2003, 92, 2341.
4. El Kholdi, O.; Lecamp, L.; Lebaudy, P.; Bunel, C.; Alexandre, S. J Appl Polym Sci 2003, 92, 2803.
5. Huck, W. T. S.; Yan, L.; Strook, A.; Haag, R.; Whitesides, G. M. Langmuir 1999, 15, 6862.
6. Zhou, F.; Liu, W.; Hao, J.; Xu, T.; Chen, M.; Xue, Q. Adv Funct Mater 2003, 13, 938.
7. Zhao, X. M.; Wilbur, J. L.; Whitesides, G. M. Langmuir 1996, 12, 3257.
8. Love, J. C.; Wolfe, D. B.; Chabinyc, M. L.; Paul, K. E.; Whitesides, G. M. J Am Chem Soc 2002, 124, 1576.
9. Xia, Y.; Mrksich, M.; Kim, E.; Whitesides, G. M. J Am Chem Soc 1995, 117, 7576.
10. Bietsch, A.; Michel, B. J Appl Phys 2000, 88, 4310.
11. Eberhardt, A. S.; Nyquist, R. M.; Parikh, A. N.; Zawodzinski, T.; Swanson, B. I. Langmuir 1999, 15, 1595.
12. Delamarche, E.; Hoole, A. C. F.; Michel, B.; Wilkes, S.; Despont, M.; Welland, M. E.; Biebuyck, H. J Phys Chem B 1997, 101, 9263.
13. Biebuyck, H. A.; Larsen, N. B.; Delamarche, E.; Michel, B. IBM J Res Dev 1997, 45, 159.
14. Delamarche, E.; Schmid, H.; Bietsch, A.; Larsen, N. B.; Rothuizen, H.; Michel, B.; Biebuyck, H. A. J Phys Chem B 1998, 102, 3324.
15. Xia, Y.; Kim, E.; Whitesides, G. M. J Electrochem Soc 1996, 143, 1070.
16. Shah, R. R.; Merreceyes, D.; Hussemann, M.; Rees, I.; Abbott, N. L.; Hawker, C. J.; Hedrick, J. L. Macromolecules 2000, 33, 597.
17. Jones, D. M.; Huck, W. T. S. Adv Mater 2001, 13, 1256.
18. Kim, J. B.; Huang, W.; Bruening, M. L.; Baker, G. L. Macromolecules 2002, 35, 5410.
19. Boyes, S. G.; Brittain, W. J.; Weng, X.; Cheng, S. Z. D. Macromolecules 2002, 35, 4960.
20. Delamarche, E.; Geissler, M.; Wolf, H.; Michel, B. J Am Chem Soc 2002, 124, 3834.